AtNFXL1, an Arabidopsis homologue of the human transcription factor NF-X1, functions as a negative regulator of the trichothecene phytotoxin-induced defense response

the plant journal

AtNFXL1, an *Arabidopsis* homologue of the human transcription factor NF-X1, functions as a negative regulator of the trichothecene phytotoxin-induced defense response.

Journal:	*The Plant Journal*
Manuscript ID:	TPJ-00751-2007.R1
Manuscript Type:	Full Paper
Date Submitted by the Author:	n/a
Complete List of Authors:	Asano, Tomoya; Kanazawa University, Advanced Science Research Center Masuda, Daisuke; Kanazawa University, ASRC Yasuda, Michiko; RIKEN, Environmental Molecular Biology Laboratory Nakashita, Hideo; RIKEN, Environmental Molecular Biology Laboratory Kudo, Toshiaki; RIKEN, Environmental Molecular Biology Laboratory Kimura, Makoto; RIKEN, Discovery Research Institute (DRI), Plant & Microbial Metabolic Engineering Research Unit Yamaguchi, Kazuo; Kanazawa University, ASRC Nishiuchi, Takumi; Kanazawa university, ASRC
Key Words:	trichothecene, phytotoxin, microarray, transcription factor, Fusarium, defense response, SA biosynthesis

AtNFXL1, an *Arabidopsis* homologue of the human transcription factor NF-X1, functions as a negative regulator of the trichothecene phytotoxin-induced defense response.

Tomoya Asano[1, 2], Daisuke Masuda[1], Michiko Yasuda[3], Hideo Nakashita[3], Toshiaki Kudo[3], Makoto Kimura[4], Kazuo Yamaguchi[1, 5] and *Takumi Nishiuchi[1, 5]

[1]Division of Functional Genomics, Advanced Science Research Center, Kanazawa University, 13-1 Takaramachi, Kanazawa 920-0934, Japan; [2]Shigeta Animal Pharmaceuticals Inc., 4569-1, Komoridani, Oyabe City, Toyama Prefecture, 932-0133 Japan; [3]Environmental Molecular Biology Laboratory, RIKEN, 2-1 Hirosawa, Wako, Saitama 351-0198, Japan; [4]Plant & Microbial Metabolic Engineering Research Unit, Discovery Research Institute (DRI), RIKEN, 2-1 Hirosawa, Wako, Saitama 351-0198, Japan; [5]Division of Life Science, Graduate School of Natural Science and Technology, Kanazawa University, Kanazawa 920-1192, Japan

*Author for correspondence (e-mail: tnish9@kenroku.kanazawa-u.ac.jp)

total word count: **7,134**

Running title: Trichothecene-inducible *AtNFXL1* gene

key words: phytotoxin, trichothecene, transcription factor, defense response

Abstract

Trichothecenes are a closely related family of phytotoxins produced by phytopathogenic fungi. In *Arabidopsis*, expression of *AtNFXL1*, a homologue of the putative human transcription repressor *NF-X1*, was significantly induced by application of type A trichothecenes, such as T-2 toxin. An *atnfxl1* mutant growing on medium lacking trichothecenes showed no phenotype, whereas a hypersensitivity phenotype was observed in T-2 toxin-treated *atnfxl1* mutant plants. Microarray analysis indicated that several defense-related genes (i.e. *WRKYs, NBS-LRRs, EDS5, ICS1,* etc.) were upregulated in T-2 toxin-treated *atnfxl1* mutant compared to wild type plants. In addition, enhanced salicylic acid (SA) accumulation was observed in T-2 toxin-treated *atnfxl1* mutant plants, which suggests that *AtNFXL1* functions as a negative regulator of these defense-related genes via an SA-dependent signaling pathway. We also found that expression of *AtNFXL1* was induced by SA and flg22 treatment. Moreover, the *atnfxl1* mutant was less susceptible to a compatible phytopathogen, *Pseudomonas syringae* pv. tomato strain DC3000 (*Pst* DC3000). Taken together, these results indicate

that *AtNFXL1* plays an important role in the trichothecene response, as well as the general defense response in *Arabidopsis*.

Introduction

Trichothecenes are a major type of mycotoxin, and are important in human health due to the risk of ingesting contaminated food (Kimura *et al*., 2006). Phytopathogenic fungi capable of producing trichothecenes are found throughout the world, and include certain species of *Fusarium*, *Myrotherium* and *Stachybotrys* (Eudes *et al*., 2001). The production of mycotoxins by these species of phytopathogenic fungi is determined by genetic factors and environmental growth conditions. Trichothecenes have a sesquiterpenoid ring structure, and can be classified according to the presence or absence of characteristic functional groups (Shifrin and Anderson, 1999). Type A trichothecenes, such as T-2 toxin, and type B trichothecenes, such as deoxynivalenol (DON), are natural contaminants of certain agricultural commodities, as well as commercial foods (Sudakin, 2003). Among the trichothecenes, type A trichothecenes are highly toxic at low concentrations.

Trichothecenes inhibit peptidyltransferase activity in eukaryotic cells by binding to the 60S ribosomal subunit. The antiproliferative activity of trichothecenes is presumed to be a consequence of their ability to inhibit protein synthesis (Shifrin and

Anderson, 1999). Thus, trichothecenes also function as phytotoxins. Specific disruption of a trichothecene synthase gene (*Tri5*) in *F. graminearum* resulted in a strain that was less virulent in the infection of wheat compared to wild type strains (Desjardins *et al*., 2000). For this reason, Desjardins *et al*. have suggested that in certain *Fusarium* species, trichothecenes act as virulence factors in the infection of plants (Desjardins *et al*., 2000). Trichothecene-producing *Fusarium* species have strain-specific trichothecene metabolite profiles (Ward *et al*., 2002), and these trichothecene chemotypes are also believed to play a role in the virulence of individual strains of *Fusarium*.

Recently, we reported that type A trichothecenes, such as T-2 toxin, have an elicitor-like activity in *Arabidopsis thaliana* at a concentration of 1 μM (Nishiuchi *et al*., 2006). Type A trichothecene-inducible lesions were also formed in SA-, jasmonic acid (JA)- and ethylene (ET)-mutants, and in SA-deficient *NahG* transgenic plants (Nishiuchi *et al*., 2006). These results implied that T-2 toxin-induced cell death has little to do with these host defense pathways; rather, the toxin contributes directly to the virulence of necrotrophic phytopathogens. In contrast to T-2 toxin, 10 μM DON inhibited protein translation in *Arabidopsis* cells, whereas it failed to activate the

elicitor-like signaling pathway (Nishiuchi *et al*., 2006), which suggests that *Fusarium* utilizes DON as a non-defense-inducing translational inhibitor during the spread of disease in host plants (Bai *et al*., 2001). Thus, the role of type B trichothecenes in virulence might be different from that of type A trichothecenes. Urban *et al*. reported that the DON-producing, wheat-attacking fungal pathogens *F. graminearum* and *F. culmorum* can infect the flowers of *Arabidopsis* contaminated with DON (Urban *et al*., 2002).

We recently reported that *AtNFXL1* is upregulated in T-2 toxin-treated *Arabidopsis* (Masuda *et al*., 2007). *AtNFXL1* encodes a putative transcription factor with similarity to the human transcription repressor NF-X1 (Lisso *et al*., 2006). Human NF-X1 was identified as a binding factor for the conserved X1 box regulatory element in the proximal promoters of class II *MHC* genes, and contains a nuclear localization signal (NLS), a RING-CH finger domain, several NF-X1-type zinc (Zn) finger domains, and an R3H domain (Song *et al*., 1994). Song *et al*. suggested that NF-X1 is involved in regulating disease states by suppressing the expression of class II *MHC* genes (Song *et al*., 1994). The RING-CH finger domain is implicated in the targeting of proteins for

ubiquitination (Lorick *et al*., 1999). The yeast *NF-X1* homologue, *FAP1*, was identified in a genetic screen for suppressors of rapamycin toxicity (Kunz *et al*., 2000). FAP1 interacted physically with a FK506-binding protein 12 (FKBP12) *in vivo* and *in vitro*, and suppressed the cytotoxic effects of rapamycin (Kunz *et al*., 2000). Strombakis *et al*. suggested that the *Drosophila NF-X1* homologue*, shuttle craft (stc),* is essential for embryogenesis by regulating the activity of a subset of genes that play a role in either the guidance or spatial maintenance of axon tracts (Strombakis *et al*., 1996). Taken together, these results suggest that the NF-X1 family of proteins has unique functions in different organisms.

In this paper, we demonstrated that *atnfxl1* mutant plants exhibit a hypersensitivity phenotype to a type A trichothecene, T-2 toxin. Microarray analysis revealed that many defense-related genes are upregulated in the *atnfxl1* mutant in the presence of trichothecenes, compared to wild type plants. High levels of SA accumulated in T-2 toxin-treated *atnfxl1* mutant plants compared to wild type plants, which suggests that *AtNFXL1* functions as a negative regulator of defense-related genes via an SA-dependent signaling pathway. In addition, we found that the expression of *AtNFXL1*

is induced by application of SA. Moreover, the *atnfxl1* mutant was less susceptible to the compatible phytopathogen *Pst* DC3000. Thus, *AtNFXL1* also appears to play an important role in the defense response to compatible phytopathgens in *Arabidopsis*.

Results

AtNFXL1 belongs to the NF-X1 family of proteins

Based on its predicted amino acid sequence, *AtNFXL1* encoded a protein with a molecular weight of 130 kDa that has similarity to the human transcription repressor NF-X1 (Supplemental Figures 1a and b). AtNFXL1 contains several functional regions and domains, including an NLS, a RING-CH finger domain, and nine NF-X1-type Zn finger domains (Supplemental Figure 1a). These domains are also conserved in *Oryza sativa* OsNF-X1, *Homo sapiens* NF-X1, *Drosophila melanogaster* STC, and *Saccharomyces cerevisiae* FAP1. The R3H domain, which is involved in binding of single stranded RNA, is present only in NF-X1 family proteins of non-plant eukaryotes (Supplemental Figure 1a). Phylogenetic analysis indicated that plant NF-X1-like proteins are more closely related to human NF-X1 than to FAP1 or STC (Supplemental

Figure 1b). *AtNFXL1* contains an intron in its 5'UTR (data not shown). The NF-X1-type Zn finger domains are unique motifs, and the Zn finger repeats are conserved in AtNFXL1 (Supplemental Figure 1c) . It has been reported that a green fluorescent protein (GFP)-AtNFXL1 fusion protein localizes to the nucleus in onion epidermal cells (Lisso et al., 2006). We also examined the localization of a GFP-AtNFXL1 fusion protein in *Arabidopsis*, and found that GFP-AtNFXL1 localizes to the nucleus in *Arabidopsis* T87 suspension cultured cells (Supplemental Figure 2).

The *atnfxl1* mutant displays a hypersensitivity phenotype to the type A trichothecene, T-2 toxin.

We recently demonstrated that *AtNFXL1* is a trichothecene-inducible gene (Masuda *et al*., 2007). To determine the function of *AtNFXL1*, we investigated the trichothecene response of *atnfxl1* (*atnfxl1-1*) mutant plants. The *atnfxl1-1* mutant was generated by transferred-DNA (T-DNA) insertion at position +2,082 (relative to the first basepair of the initiation codon at +1) of the open reading frame of *AtNFXL1* (Munich Information Center for Protein Sequence designation At1g10170), as previously described (Figure

1a; Lisso *et al*., 2007). In wild type plants, *AtNFXL1* was weakly expressed in the absence of T-2 toxin, whereas it was induced by 1 μM T-2 toxin treatment, as previously reported (Figure 1b; Masuda et al., 2007). In the *atnfxl1* mutant, we observed a truncated transcript of *AtNFXL1* (Figure 1b). The deduced amino acid sequence of the truncated mRNA in the *atnfxl1* mutant lacked two of the nine NF-X1-type Zn finger domains. Therefore, it is likely that the truncated form of *atnfxl1* mRNA in mutant plants does not encode a functional protein. The *atnfxl1* mutant exhibited no apparent phenotype on MS agar medium alone (without trichothecene) compared to wild type plants (Figures 1c and 1d). In addition, general phenotypes, such as growth rate, organ development, and morphology of untreated *atnfxl1* mutant were similar to wild type plants (data not shown). In contrast, *atnfxl1* mutant exhibited a severe growth defect on MS medium containing 0.1 μM T-2 toxin (Figures 1c and 1d). As previously reported (Masuda et al., 2007), cell death was not induced when seedlings were transferred to 0.1-1 μM T-2 toxin-containing medium. The T2 segregation ratio of the toxin-hypersensitivity phenotype was nearly 1:3 in self-pollinated offspring of heterozygous *atnfxl1* plants, which indicated that the mutation was inherited as a single

recessive trait. As shown in Figure 1d, the growth defects of DON-treated *atnfxl1* mutant were similar to DON-treated wild type plants.

To determine whether the T-2 toxin-sensitive phenotype of *atnfxl1* mutant plants was due to a defect in *AtNFXL1*, we carried out a complementation analysis. Introduction of a complementation plasmid containing the promoter and the coding sequence of *AtNFXL1* (*AtNFXL1 promoter::AtNFXL1*, see Experimental Procedures) into *atnfxl1* mutant plants clearly rescued the hypersensitivity phenotype in the presence of 0.1 μM T-2 toxin in 7 of 8 plant lines (Figures 1c and 1d). These results demonstrated that the hypersensitivity to T-2 toxin of *atnfxl1* mutant plants was due to a defect in *AtNFXL1*.

Defense-related genes are upregulated in trichothecene-treated *atnfxl1* mutant plants.

We performed a transcriptome analysis of approximately 14,880 genes to obtain the expression profiles of putative *AtNFXL1*-regulated genes. This analysis was carried out using two independent wild-type plants, and two independent mutant plant lines. As

seen in Figure 1b, *atnfxl1* mutant plants displayed no visible phenotype in the absence of trichothecenes. In accordance with this result, none of the genes we examined were upregulated more than 3-fold in *atnfxl1* mutant plants compared to wild type plants in the absence of trichothecenes (data not shown). A single gene was down-regulated greater than 3-fold in *atnfxl1* mutant plants compared to wild type plants (data not shown). These results indicated that in the absence of trichothecenes, *AtNFXL1* has a minor effect on the global regulation of gene expression.

In contrast, in 1 μM T-2 toxin-treated *atnfxl1* mutant plants, 130 genes were upregulated greater than 3-fold compared to T-2 toxin-treated wild type plants (Table 1). As seen in Table 1, 18 of the upregulated genes were putative transcriptional regulators. In particular, 8 *WRKY* family genes were upregulated in T-2 toxin-treated *atnfxl1* mutant plants. WRKY transcription factors play pivotal roles in the plant defense response (Eulgem *et al*., 2000), and expression of some *WRKY* family genes confers enhanced disease resistance in *Arabidopsis* and tobacco (Asai *et al*., 2002; Liu *et al*., 2004; Chen and Chen, 2002). .

The largest category of putative *AtNFXL1*-regulated genes (28 genes) encoded

cellular communication and signal transduction factors (Table 1). This category included 9 genes that encode serine/threonine protein kinases, including a Pto-like kinase, and 7 genes that encode receptor-like protein kinases, which suggests that these genes function as components of *AtNFXL1*-regulated defense signaling pathways. Several defense-related genes also appeared to be regulated by *AtNFXL1*, including 5 genes that encode disease resistance proteins, as well as *EDS5* and *ICS1*. *EDS5* was identified as an essential component of SA-dependent signaling in resistance to *Pst* DC3000 in *Arabidopsis* (Nawrath *et al*., 2002). *ICS1* encodes an isochorismate synthase, and is required for biosynthesis of SA (Wildermuth *et al*., 2001). These results suggested that *AtNFXL1* is involved in SA-dependent defense signaling pathways in trichothecene-treated *Arabidopsis*.

Table 2 lists the genes that were down-regulated greater than 3-fold in T-2 toxin-treated *atnfxl1* mutant plants compared to wild type plants. The list of genes included *LHCB2-4*, which suggests that hyperactivation of the defense response affects the expression of phytosynthesis-related genes.

To validate the results of the microarray analysis, we selected 6 genes that

were upregulated, and 1 gene that was down-regulated in T-2 toxin-treated *atnfxl1* mutant plants, and analyzed them by real time PCR. As shown in Table 3, we obtained similar results using real time PCR, although the magnitude of the expression change of some of the genes was greater than what was observed by microarry analysis.

Enhanced SA accumulation in T-2 toxin-treated *atnfxl1* mutant plants.

Microarray analysis revealed that defense-related genes, including genes involved in SA biosyntheis, were upregulated in *atnfxl1* mutant compared to wild type plants. *PR-1* (At2g14160), which is regulated in an SA-dependent manner, was not present on the Agilent *Arabidopsis 1* microarray. When we examined the expression of *PR-1* by RT-PCR, we found that *PR-1* was weakly induced 24 hours (hr) after T-2 toxin treatment in both wild type and *atnfxl1* mutant, as previously described (Masuda et al., 2007). The T-2 toxin-induced expression of *ICS1* was enhanced in *atnfxl1* mutant plants compared to wild type plants (Figure 2a). These results suggested that SA biosynthesis is activated in *atnfxl1* mutant plants. We next measured free and total SA levels in wild type and *atnfxl1* mutant plants in the presence or absence of T-2 toxin. As seen in

Figures 2b and 2c, T-2 toxin-induced SA accumulation was enhanced in *atnfxl1* mutant plants compared to wild type plants. Taken together, these results suggested that enhanced SA accumulation in *atnfxl1* mutant plants leads to the induction of defense-related genes (Table 1).

SA and flg22 activate the transcription of *AtNFXL1*.

To investigate the expression pattern of *AtNFXL1* in more detail, we generated transgenic plants carrying an *AtNFXL1 promoter::β-glucuronidase (GUS)* gene fusion construct. As shown in Figure 3a, in seedlings of *AtNFXL1::GUS* transformants, in the absence of trichothecene, GUS activity was present in the vascular bundle and meristematic tissue. *AtNFXL1* promoter activity was increased up to approximately 18-fold by 0.1 μM T-2 toxin treatment compared to mock (no trichothecene) treatment (Figures 3a, 3b and 3d). Treatment with 2.5 μM DAS induced an 8-fold increase in promoter activity, while treatment with 10 μM DON resulted in a 3-fold induction of promoter activity (Figure 3d). Since *AtNFXL1* is predicted to play a role in defense signaling, including SA-dependent signaling, we also investigated whether other

elicitors and defense-related signals affected the expression of *AtNFXL1*. *AtNFXL1* promoter activity was increased approximately 5-fold by flg22, a peptide elicitor derived from phytopathogenic bacteria (Figure 3d). SA treatment induced an approximate 40-fold increase in GUS activity in *AtNFXL1* promoter::*GUS* transformants (Figure 3a, 3c, and 3d), and 1-aminocyclopropane-1-carboxylic acid (ACC) and methyl jasmonate (MeJA) induced a 2.5-fold and 3.2-fold increase in promoter activity, respectively (Figure 3d). These results suggested that *AtNFXL1* plays a role not only in the action of trichothecenes, but also in the general defense response of *Arabidopsis*.

The *atnfxl1* mutant is less susceptible to *Pst* DC3000.

To determine whether *AtNFXL1* is involved in disease resistance to phytopathogens, wild type and *atnfxl1* mutant plants were inoculated with the compatible pathogen *Pst* DC3000. As shown in Figure 4a, the growth of *Pst* DC3000 in *atnfxl1* mutant plants was slower than in wild type plants, which indicated that *atnfxl1* mutant plants are less susceptible to *Pst* DC3000. The reduced susceptibility to the compatible pathogen *Pst*

DC3000 was not observed after complementation with wild type *AtNFXL1* (Figure 4b). These results indicated that the reduced susceptibility phenotype of *atnfxl1* mutant is due to a defect in *AtNFXL1*. These results also provided further evidence that *AtNFXL1* functions not only in the trichothecene response, but also in the general defense response in *Arabidopsis*.

Discussion

The action of trichothecenes in host plants can not simply be attributed to general toxicity, such as inhibition of translation. For example, we previously reported that some type A trichothecenes have an elicitor-like activity in infiltrated *Arabidopsis* leaves (Nishiuchi *et al*., 2006). Both DON and DAS preferentially inhibit root elongation, whereas T-2 toxin-treated seedlings exhibit dwarfism and aberrant morphological changes (Masuda *et al*., 2007). In contrast, neither feature was observed in seedlings treated with a general translational inhibitor, cycloheximide (CHX). These results indicate that the action of trichothecenes in plants differs significantly according to molecular species, and highlight the importance of examining the site of

action of trichothecenes in host plants. In this study, we demonstrated that *AtNFXL1* is an important regulator of trichothecene action in *Arabidopsis*. Our results may provide a key to understanding the molecular mechanism of phytotoxic trichothecenes in host plants.

AtNFXL1 was upregulated not only by type A trichothecenes, but also SA and flagellin (Figure 3). SA, in particular, drastically induced the expression of *AtNFXL1*. We identified several putative *AtNFXL1*-regulated genes using microarray analysis, including many defense-related genes, such as *WRKYs*, *RLKs*, and *NBS-LRRs* (Table 1). Since these genes are putative regulators of defense signaling pathways in *Arabidopsis*, it is likely that *AtNFXL1* functions as a component of these pathways, particularly the SA-dependent signaling pathway. Dong *et al*. reported that many of the *Arabidopsis WRKY* family genes are induced by pathogen-infection and/or SA treatment, including the putative *AtNFXL1*-regulated *WRKY* genes that we identified in the current study (Dong *et al*., 2003). Overexpression of *WRKY6* and *WRKY53* results in a dwarfed phenotype in transgenic plants (Robatzek and Somssich, 2002; Ulker and Somssich, 2004); thus, upregulation of these two genes in *atnfxl1* mutant plants may contribute to

the severe growth defects of these plants in the presence of type A trichothecenes. *EDS5*, which is an essential component of SA-dependent signaling in resistance to *Pst* DC3000 in *Arabidopsis* (Nawrath *et al*., 2002), and *ICS1*, which encodes an isochorismate synthase that is required for biosynthesis of SA (Wildermuth *et al*., 2001), were also upregulated in T-2 toxin-treated *atnfxl1* mutant plants. In fact, *AtNFXL1* appeared to be involved in the negative regulation of SA biosynthesis in response to T-2 toxin (Figures 2b and 2c), and possibly other elicitors and infectious pathogens as well. In this manner, *AtNFXL1* may act to suppress the hyperactivation of defense responses to elicitors or pathogens. In support of this hypothesis, *atnfxl1* mutant plants displayed less susceptibility to the compatible phytopathogen *Pst* DC3000 (Figure 4). The *atnfxl1* mutant could not repress the defense response induced by type A trichothecenes, resulting in severe growth defects in trichothecene-treated *Arabidopsis* seedlings. This phenotype was similar to that of the constitutive defense response mutant *cpr1* (Bowling *et al*., 1994).

Lisso *et al*. reported that *AtNFXL1* is induced by salt stress and osmotic stress, and that *atnfxl1* mutant plants display reduced survival rates after salt stress compared

to wild type plants (Lisso *et al*., 2006). In addition, certain salt-responsive genes, such as *COR15A, KIN1,* and *RAB18*, showed weaker expression levels in *atnfxl1* mutant under salt stress compared to the wild type plants (Lisso *et al*., 2006). The expression of *COR15A, KIN1,* and *RAB18* is also induced by ABA in *Arabidopsis* (Baker *et al*., 1994; Kurkela and Franck, 1990; Lang and Palva, 1992). In contrast, transgenic *35S::AtNFXL1* plants exhibited an enhanced survival rate under salt stress, and higher expression of salt-responsive genes. These results indicate that AtNFXL1 functions as a positive regulator of expression of salt-inducible genes under salt stress conditions (Figure 5). We demonstrated that AtNFXL1 negatively regulates the expression of several defense-related genes in trichothecene-treated *Arabidopsis* plants (Figure 5). Thus, it seems likely that AtNFXL1 has opposing functions in the salt stress response and defense response. ABA plays a negative role in defense signaling pathways, including SA-, JA-, and ET-dependent signaling pathways (Mauch-Mani and Mauch, 2005). Therefore, AtNFXL1-controlled stress signaling might depend on components of both the defense and the ABA signaling pathways.

Human NF-X1 binds directly to *cis*-elements in target genes *in vitro*, and

regulates transcription through these elements *in vivo* (Song *et al*., 1994; Gewin *et al*., 2004). However, activation or repression domains have not been identified in any NF-X1 family protein to date. AtNFXL1 contains a RING-CH finger domain, which is a binding motif for the ubiquitin-conjugating enzyme E2s (Lorick *et al*., 1999). Thus, AtNFXL1 may function as a repressor by mediating the degradation of its binding partners. NF-X1 exists as two isoforms: NFX1-123 and NFX1-91. Recently it was shown that NFX1-123 and c-Myc function cooperatively to activate the *hTERT* promoter, whereas NFX1-91 repressed *hTERT* promoter activity (Gewin *et al*., 2004). These results raise the possibility that NF-X1 family proteins function as negative regulators of their targets. In support of this hypothesis, Lisso *et al*. reported that another *Arabidopsis* NF-X1-like protein, AtNFXL2, is a negative regulator of the salt stress response (Lisso *et al*. 2006). It has been reported that some elicitor-responsive RING-H2 finger proteins have roles in plant defense signaling pathways (Takai *et al*., 2002; Serrano and Guzman, 2004). Thus, the RING-CH finger domain of AtNFXL1 may have a role in regulating the stability of defense-related target proteins.

NF-X1 represses INF-γ-inducible expression of class II *MHC* genes in

INF-γ-treated cells, whereas it has no effect on the expression of these genes in untreated cells (Song *et al*. 1994). In addition, *FAP1* was identified as a suppressor of rapamycin toxicity. FAP1 physically interacts with FKBP12 *in vivo* and *in vitro* to suppress the function of rapamycin, and FAP1 is targeted to the nucleus by rapamycin treatment. In the current study, we showed that *atnfxl1* mutant plants are hypersensitive to the type A trichothecene, T-2 toxin (Figure 2), but display no phenotype in the absence of chemical. Taken together, these results suggest that *AtNFXL1, NF-X1,* and *FAP1* are together involved responding to chemical stimuli, but have no apparent phenotype in the absence of chemicals.

In summary, we have presented evidence that the trichothecene-inducible gene *AtNFXL1* negatively regulates many defense-related genes, at least in part through the regulation of SA biosynthesis (Figure 5). Additional studies that investigate how *atnfxl1* mutant behave when challenged by necrotrophic pathogens, such as trichothecene-producing fungi, are needed. While we have not established a *Fusarium-Arabidopsis* pathosystem for interaction studies, it has been reported that *A. thaliana* is susceptible to type B DON-producing species of *Fusarium* (Uraban *et al*.,

2002). Studies to determine whether *Arabidopsis* is susceptible to T-2 toxin-producing fungi such as *Fusarium spoichiomerdes* are ongoing, and will further our understanding of the role of *AtNFXL1* in host plant resistance to trichothecene-producing fungi.

Experimental procedures

Plant growth and trichothecene treatment

The Columbia (Col-0) ecotype of *Arabidopsis thaliana* (L.) Heynh was used as the wild type plant in this study. Sterile seeds were sown on Murashige and Skoog (MS) medium that contained 3% (w/v) sucrose and 0.3% (w/v) gelrite (San-Ei Gen F.F.I., Inc.) in plastic petri dishes, and then stratified for 2 days (d) at 4ºC in the dark. Plants were grown at 22ºC under long day conditions (16 hours (hr) light/8 hr dark cycles or continuous light) in a growth chamber. A T-DNA insertion mutant (*atnfxl1-1*) of *AtNFXL1* (N501399) was obtained from the *Arabidopsis* Biological Resource Center, Ohio State University, Columbus, Ohio. For trichothecene or defense-related molecule treatment, *Arabidopsis* seeds were sown on MS agar medium containing the indicated

substance, and plants were continuously grown. Alternatively, *Arabidopsis* plants were first grown on MS medium without treatment, and then transferred to MS medium containing the indicated molecules. Additional details of each treatment are noted in the text or figure legends.

Generation of transgenic plants

A region of the *AtNFXL1* promoter (-795 basepairs relative to the start site at +1) was amplified by PCR using primers 1 (5'-GCGAAGCTTACTGGTTAGATTGGTTTAAG-3') and 2 (5'-GCGGGATCCATTCTGCCTTGACTCCACAAA-3'), and then introduced into the *Hin*dIII and *Bam*HI sites of pBI121. For complementation analysis, a *Sac*I fragment of the F14N23 BAC clone containing the promoter region and coding region of *AtNFXL1* was introduced into the *Sac*I site of pSMAH621. Plasmids were introduced into wild type or *atnfxl1* mutant plants by *in planta* transformation, as previously described (Asano *et al.*, 2004). Several independent transformants were obtained, and detailed analysis was carried out on T2 and T3 plants.

Reverse transcription-polymerase chain reaction (RT-PCR) analysis

In a total volume of 20 µl, cDNAs were synthesized from 1 µg of total RNA using SuperScript III reverse transcriptase (Invitrogen) with a oligo$(dT)_{16}$ primer, and then 0.5 µl of the cDNA was subsequently used for PCR analysis. All PCR reactions were performed in a total volume of 10 µl, for 24-28 cycles under the following conditions: denaturation, 94ºC, 30 seconds (s); annealing, 55ºC, 30 s; extension, 72ºC, 30 s. The following gene-specific primers were used: *AtNFXL1 120-438*, 5'-CCCATATGCCTCCTAATACAGATAGAAATTC-3' and 5'-ACGTCGACCTCAGGAGCATTATTTCTTCTATG-3'; *AtNFXL1 2363-3568*, 5'-CGCCATATGCATGTGGTCGTATAACCGCTA-3' and 5'-GACGTCGACCTCACATACCTTCTCCCAGT-3'; *ACT2/8*, 5'-CATCACACTTTCTACAATGAGCT-3' and 5'-CGACCTTAATCTTCATGCTGC-3'.

Real time PCR analysis

Real time PCR was performed using the LightCycler Quick System 350S (Roche

Diagnostics K.K., Tokyo, Japan) with SYBR Premix Ex Taq (TAKARA BIO INC., Shiga, Japan). The PCR reaction contained 1 x SYBR Premix Ex Taq, 0.2 μM of each primer, and the appropriate dilution of cDNA in a final volume of 20 μl. The following PCR program was used: initial denaturation, 95ºC, 10 s; 40 cycles of 95ºC, 5 s and 60ºC, 20 s with a temperature transition rate of 20ºC/s; melting curve analysis, 95ºC, 0 s, 65ºC, 15 s, and an increase to 95ºC with a temperature transition rate of 0.1ºC/s. To generate a standard curve, homologous standards were used as external standards in all experiments. Template DNA was quantified using the second derivative maximum methods of the LightCycler Software Ver.3.5 (Roche Diagnostics), then normalized to *Actin2/8* mRNA. The following gene-specific primers were used: At5g25930, 5'-ACATTGCTCCAGAATACGC-3' and 5'-CATCGCCTCAGTCGTG-3'; *WRKY15*, 5'-TGCTCGAAGAAAAGAAAGATAAAAC-3' and 5'-AGTAACAATCAACATGGACG-3'; At5g41750, 5'-AAAGGAACAGGTACTGAATCT-3' and 5'-TGTAGTAACCTAACAGGAGGTAT-3'; *Hsf21*, 5'-GCCAGCTTAACACATATGGT-3' and 5'-TCTGATTATTCATTCTCACTCGT-3'; *EDS5*, 5'-GGTACATTGCTGGCGG-3'

and 5’-GTATGCCTCCAGGCGA-3’; At3g60420, 5’-AGATCAAGGTGGCTATTGAA-3’ and 5’- CTCAAAGGCTTGTGCAG-3’; *MYB29*, 5’-TTCTCGCGGCAACAAG-3’ and 5’- GCTGGTTATCTCCGGTACA-3’; *Actin2/8*, 5′-GGTAACATTGTGCTCAGTGGTGG-3′ and 5′-AACGACCTTAATCTTCATGCTGC-3′; *ICS1*, 5’-ATGAGATTCAGCCTCGCTGT-3’ and 5’-TGATGGATCTCCAATCGTCA-3’; *PR-1*, 5’- ATTACTTCATTAGTATGGCTTCT-3’ and 5’-CTTGTCTGGCGTCTCC-3’. All kits were used according to the manufacture’s protocols.

Microarray analysis

Ten-day-old seedlings of wild type and *atnfxl1* mutant plants were grown on MS plates and harvested after mock or 1 μM T-2 toxin treatment for 24 hr. Samples for microarray analysis were taken at the middle stage of the light period. Total RNA was prepared from T-2 toxin-treated or untreated *Arabidopsis* shoots using a guanidine hydrochloride–phenol-chloroform extraction method, as previously described (Nishiuchi et al., 2006). The quality of RNA was assessed using the RNA 6000 Nano

LabChip Kit (Bioanalyzer 2100; Agilent Technologies, Inc.), then the microarray experiment was carried out using the Agilent *Arabidopsis* 1 Oligo Microarray (Agilent Technologies, Inc.), according to the Agilent 60-mer Oligo Microarray Processing Protocol (Agilent Technologies, Inc.). Total RNA (5 μg) from wild type and *atnfxl1* mutant plants was used to prepare Cy3- and Cy5-labeled cDNAs, respectively, using a Fluorescent Direct Labeling Kit (Agilent Technologies). The two different fluorescently labeled cDNAs were combined and purified using an RNeasy RNA purification Kit (Qiagen Inc.). Following hybridization and washing, arrays were scanned under maximum laser intensity with both the Cy3 and Cy5 channels using an Agilent microarray scanner (G2565BA; Agilent Technologies). Images were analyzed with Feature Extraction Software (version 7.0; Agilent Technologies). Two independent experiments were carried out using different plant samples to demonstrate the reproducibility of the microarray analysis. Upregulated or downregulated genes were designated as such if a 3-fold or greater change in expression relative to wild type plants was observed. All changes in gene expression were statistically significant ($P<0.01$).

SA measurement.

SA and SAG levels in mock- or T-2 toxin-treated samples were measured as described previously (Nakashita et al., 2002).

GUS assays

For GUS staining, plants were continuously treated with the indicated substance for 8 days. The *AtNFXL1 promoter::GUS* transformants were fixed in 90% acetone at -20^{o}C, then incubated in a solution containing 0.5 mM $K_4[Fe(CN)_6]$, 0.5 mM $K_4[Fe(CN)_6]\cdot 3H_2O$, 1 mM EDTA, and 1 mM X-Gluc in 100 mM phosphate buffer (pH7.2) at 37 ^{o}C for 2 hr. Samples were destained by a series of ethanol washes. For the fluorometric assay, 8-day-old plants were transferred to medium containing the indicated substance, incubated for 24 hr, and then subjected to quantification of GUS activity. The fluorometric assay of GUS activity was performed as previously described (Nishiuchi *et al*., 1995).

Bacterial Infection

The *Pst*DC3000 infection assay was performed as previously described (Yasuda *et al*., 2003).

Visualization of the GFP-AtNFXL1 fusion protein.

The entire coding region of *AtNFXL1* was amplified from cDNA by PCR using the following primers: 5'-CACCATGAGCTTTCAAGTCAGGCG-3' and 5'-TCACTCACATACCTTCTCCC-3'. The PCR fragment was inserted into the pENTR™/D-TOPO entry vector (Invitrogen Inc, Germany), then introduced into pH7WGF2 (Karimi et al., 2002). Protoplasts of *Arabidopsis* T87 suspension culture cells were transiently transfected with the GFP-AtNFXL1 plasmid using the polyethylene glycol (PEG) method (Abel and Theologis, 1994). GFP was visualized by microscopy (BX-50; Olympus Optical, Tokyo) using a built-in BX-FLA epifluorescent unit.

Acknowledgement

We thank Dr. Hiroaki Ichikawa for kindly providing the binary vector, pSMAH621 containing the hygromycin-resistance gene (*hpt*) as a selection marker.

References

Abel, S. and Theologis, A. (1994) Transient transformation of Arabidopsis leaf protoplasts: a versatile experimental system to study gene expression. *Plant J.* **5**, 421-427.

Asai, T., Tena, G., Plotnikova, J., Willmann, M.R., Chiu, W.L., Gomez-Gomez, L., Boller, T., Ausubel, F.M. and Sheen, J. (2002) MAP kinase signalling cascade in *Arabidopsis* innate immunity. *Nature* **415**, 977-983.

Asano, T., Yoshioka, Y., Kurei, S., Sakamoto, W., Sodmergen and Machida, Y. (2004) A mutation of the *CRUMPLED LEAF* gene that encodes a protein localized in the outer envelope membrane of plastids affects the pattern of cell division, cell differentiation, and plastid division in *Arabidopsis. Plant J.* **38**, 448-459.

Bai, G.H., Desjardins, A.E. and Plattner, R.D. (2001) Deoxynivalenol-nonproducing *Fusarium graminearum* causes initial infection, but does not cause disease spread in wheat spikes. *Mycopathologia* **153**, 91-98.

Baker, S.S., Wilhelm, K.S. and Thomashow, M.F. (1994) The 5'-region of *Arabidopsis thaliana cor15a* has *cis*-acting elements that confer cold-, drought- and ABA-regulated gene expression. *Plant Mol. Biol*. **24**, 701-713.

Bowling, S.A., Guo, A., Cao, H., Gordon, A.S., Klessig, D.F. and Dong, X. (1994) A mutation in Arabidopsis that leads to constitutive expression of systemic acquired resistance. *Plant Cell* **6**, 1845-1857.

Chen, C. and Chen, Z. (2002) Potentiation of developmentally regulated plant defense response by AtWRKY18, a pathogen-induced Arabidopsis transcription factor. *Plant Physiol*. **129**, 706-716.

Desjardins, A.E., Bai, G., Plattner1, R.D. and Proctor1, R.H. (2000) Analysis of aberrant virulence of *Gibberella zeae* following transformation-mediated complementation of a trichothecene-deficient (*Tri5*) mutant. *Microbiology* **146,** 2059-2068.

Dong, J., Chen, C. and Chen, Z. (2003) Expression profiles of the *Arabidopsis* WRKY gene superfamily during plant defense response. *Plant Mol. Biol*. **51**, 21-37.

Eudes, F., Comeau, A., Rioux, S. and Collin, J. (2001) Impact of trichothecenes on

Fusarium head blight [*Fusarium graminearum*] development in spring wheat (*Triticum aestivum*). *Can. J. Plant Pathol*. **23,** 318-322.

Eulgem, T., Rushton, P.J., Robatzek, S. and Somssich, I.E. (2000) The WRKY superfamily of plant transcription factors. *Trends Plant Sci.* **5**, 199-206.

Gewin, L., Myers, H., Kiyono, T. and Galloway, A.D. (2004) Identification of a novel telomerase repressor that interacts with the human papillovirus type-16 E6/E6-AP complex. *Genes Dev*. **18,** 2269-2282.

Kimura, M., Takahashi-Ando, N., Nishiuchi, T., Ohsato, S., Tokai, T., Ochiai, N., Fujimura, M., Kudo, T., Hamamoto, H. and Yamaguchi, I. (2006) Molecular biology and biotechnology for reduction of *Fusarium* mycotoxin contamination. *Pestic. Biochem. and Physiol.* **86**, 117-123.

Karimi, M., Inze, D. and Depicker, A. (2002) Gateway vectors for Agrobacterium-mediated plant transformation. Trends Plant Sci. **7**, 193-195.

Kunz, J., Loeschmann, A., Deuter-Reinhard, M. and Hall, M.N. (2000) FAP1, a homologue of human transcription factor NF-X1, competes with rapamycin for binding to FKBP12 in yeast. *Mol. Microbiol*. **37,** 1480-1493.

Kurkela, S. and Franck, M. (1990) Cloning and characterization of a cold- and ABA-inducible *Arabidopsis* gene. *Plant Mol. Biol*. **15**, 137-144.

Lang, V. and Palva, E.T. (1992) The expression of a *rab*-related gene, *rab18*, is induced by abscisic acid during the cold acclimation process of *Arabidopsis thaliana* (L.) Heynh. *Plant Mol. Biol*. **20**, 951-962.

Lisso, J., Altmann, T. and Mussig, C. (2006) The *AtNFXL1* gene encodes a NF-X1 type zinc finger protein required for growth under salt stress. *FEBS Lett*. **580,** 4851-4856.

Liu, Y., Schiff, M. and Dinesh-Kumar, S.P. (2004) Involvement of MEK1 MAPKK, NTF6 MAPK, WRKY/MYB transcription factors, *COI1* and *CTR1* in *N*-mediated resistance to tobacco mosaic virus. *Plant J*. **38**, 800-809.

Lorick, K.L., Jensen, J.P., Fang, S., Ong, A.M., Hatakeyama, S. and Weissman, A.M. (1999) RING fingers mediate ubiquitin-conjugating enzyme (E2)-dependent ubiquitination. *Proc. Natl. Acad. Sci*. **96,** 11364-11369.

Masuda, D., Ishida, M., Yamaguchi, K., Yamaguchi, I., Kimura, M. and Nishiuchi, T. (2007) Phytotoxic effects of trichothecenes on the growth and morphology in

Arabidopsis thaliana. *J. Exp. Bot.* 58, 1617-1626.

Mauch-Mani, B. and Mauch, F. (2005) The role of abscisic acid in plant-pathogen interactions. *Curr. Opin. Plant Biol.* **8**, 409-414.

Nawrath, C., Heck, S., Parinthawong, N. and Metraux, J.P. (2002) EDS5, an essential component of salicylic acid-dependent signaling for disease resistance in *Arabidopsis*, is a member of the MATE transporter family. *Plant Cell* **14**, 275-286.

Nishiuchi, T., Masuda, D., Nakashita, H., Ichimura, K., Shinozaki, K., Yoshida, S., Kimura, M., Yamaguchi, I. and Yamaguchi, K. (2006) *Fusarium* phytotoxin trichothecenes have an elicitor-like activity in *Arabidopsis thaliana*, but the activity differed significantly among their molecular species. *Mol. Plant Microbe Interact*. **19**, 512-20.

Nishiuchi, T., Nakamura, T., Abe, T., Kodama, H., Nishimura, M. and Iba, K. (1995) Tissue-specific and light-responsive regulation of the promoter region of the *Arabidopsis thaliana* chloroplast ω-3 fatty acid desaturase gene (*FAD7*). *Plant Mol. Biol.* **29**, 599-609.

Robatzek, S. and Somssich, I.E. (2002) Targets of AtWRKY6 regulation during plant senescence and pathogen defense. *Genes Dev*. **16**, 1139-1149.

Rogers, E.E., and Ausubel, F.M. (1997) *Arabidopsis* enhanced disease susceptibility mutants exhibit enhanced susceptibility to several bacterial pathogens and alterations in *PR-1* gene expression. *Plant Cell* **9**, 305-316.

Serrano, M. and Guzman, P. (2004) Isolation and gene expression analysis of Arabidopsis thaliana mutants with constitutive expression of *ATL2*, an early elicitor-response RING-H2 zinc-finger gene. *Genetics* **167**, 919-29.

Shifrin, V.I. and Anderson, P. (1999) Trichothecene mycotoxins trigger a ribotoxic stress response that activates c-Jun N-terminal kinase and p38 mitogen-activated protein kinase and induces apoptosis. *J. Biol. Chem*. **274,** 13985-13992.

Song, Z., Krishna, S., Thanos, D., Strominger, J.L. and Ono, S.J. (1994) A novel cysteine-rich sequence-specific DNA-binding protein interacts with the conserved X-box motif of the human major histocompatibility complex class II genes via a repeated Cys-His domain and functions as a transcriptional repressor. *J. Exp. Med*. **180,** 1763-1774.

Stroumbakis, N.D., Li, Z. and Tolias, P.P. (1996) A homolog of human transcription factor NF-X1 encoded by the *Drosophila shuttle craft* gene is required in the embryonic central nervous system. *Mol. Cell Biol*. **16,** 192-201.

Sudakin, D.L. (2003) Trichothecenes in the environment: relevance to human health. *Toxicol. Lett.* **143**. 97-107.

Takai, R., Matsuda, N., Nakano, A., Hasegawa, K., Akimoto, C., Shibuya, N. and Minami, E. (2002) EL5, a rice *N*-acetylchitooligosaccharide elicitor-responsive RING-H2 finger protein, is a ubiquitin ligase which functions *in vitro* in co-operation with an elicitor-responsive ubiquitin-conjugating enzyme, *Os*UBC5b. *Plant J.* **30**, 447-455.

Ulker, B. and Somssich, I.E. (2004) WRKY transcription factors: from DNA binding towards biological function. *Curr. Opin. Plant Biol.* **7**, 491-498.

Urban, M., Daniels, S., Mott, E. and Hammond-Kosack, K. (2002) *Arabidopsis* is susceptible to the cereal ear blight fungal pathogens *Fusarium graminearum* and *Fusarium culmorum*. *Plant J*. **32,** 961-973.

Ward, T.J., Bielawski, J.P., Kistler, H.C., Sullivan, E. and O'Donnell, K. (2002) Ancestral polymorphism and adaptive evolution in the trichothecene mycotoxin gene cluster of phytopathogenic *Fusarium. Proc. Natl. Acad. Sci.* **99**, 9278-9283.

Wildermuth, M.C., Dewdney, J., Wu, G. and Ausubel, F.M. (2001) Isochorismate synthase is required to synthesize salicylic acid for plant defence. *Nature* **414,** 562-565.

Yasuda, M., Nakashita, H., Hasegawa, S., Nishioka, M., Arai, Y., Uramoto, M., Yamaguchi, I. and Yoshida, S. (2003) *N*-cyanomethyl-2-chloroisonicotinamide induces systemic acquired resistance in *Arabidopsis* without salicylic acid accumulation. *Biosci. Biotechnol. Biochem*. **67**, 322-328.

Table 1. Upregulated genes in 1 μM T-2 toxin-treated *atnfxl1* mutant plants compared to T-2 toxin-treated wild type p

Functional	subcategory	AGI code	Descriptions	exp.1		exp.2	
				FC[B]	P value[C]	FC	P value
Cellular Communication / Signal Transduction[A]							
	protein kinase						
		At5g26920	serine threonine kinase-like protein	7.8	1.9E-05	6.0	5.5E-05
		At5g39670	serine threonine kinase-like protein	6.6	3.6E-05	4.9	1.4E-04
		At5g59680	protein kinase-like protein	4.8	3.8E-04	5.3	1.7E-03
		At4g11890	NAK-like protein kinase	5.1	1.2E-04	4.8	1.6E-04
		At4g23200	similar to serine/threonine/tyrosine-specific protein	4.7	2.0E-04	3.4	1.7E-03
		At5g06860	serine threonine kinase - like protein	3.4	1.3E-03	4.2	3.5E-04
		At5g67080	protein kinase-like protein (MAPKKK19)	4.3	3.3E-04	3.1	5.8E-03
		At5g65600	protein kinase-like protein	3.5	1.2E-03	3.3	6.4E-03
	receptor-like protein kinase						
		At5g18470	putative receptor-like protein kinase	6.3	4.2E-05	6.1	4.9E-05
		At3g25600	similar to receptor-like serine/ threonine protein kinase	3.5	1.0E-03	5.3	9.8E-05
		At4g04500	receptor-like protein kinase-like	5.7	7.6E-05	3.1	2.3E-03
		At5g25930	**receptor protein kinase-like protein**	4.2	3.6E-04	3.8	6.1E-04
		At3g47480	receptor protein kinase-like protein	4.6	2.0E-04	3.3	1.4E-03
		At4g08850	receptor protein kinase-like protein	3.3	1.5E-03	4.2	3.6E-04
		At5g39020	S-receptor kinase homolog 2 precursor	3.6	9.6E-04	3.7	1.3E-03
		At4g23280	similar to disease resistance protein kinase Pto	3.6	8.9E-04	3.6	1.9E-03
		At5g60900	serine threonine-specific protein kinase-like (RLK1)	3.9	5.6E-04	3.1	2.2E-03
	calcium-binding portein						
		At2g41100	putative calcium-binding protein (TCH3)	6.8	3.2E-05	7.5	2.1E-05
		At4g17660	hypothetical protein, EF-hand calcium-binding domain	6.0	7.3E-05	6.0	1.6E-04
		At4g27280	calcium-binding protein-like	3.4	1.4E-03	9.5	9.8E-06
		At5g42380	putative calltractin	5.9	5.6E-05	4.2	3.2E-04
		At5g25440	putative protein, EF-hand calcium-binding domain	5.0	1.3E-04	4.9	1.7E-04
	calmodulin-related porotein						
		At3g01830	calmodulin-binding-like protein	5.6	7.2E-05	6.0	5.2E-05
		At5g13320	calmodulin-related protein	5.8	6.0E-05	5.7	6.5E-05
		At4g23150	calmodulin-like protein	4.1	4.2E-04	3.2	2.2E-03
		At5g61560	calmodulin, putative	3.1	2.5E-03	4.1	4.2E-04
	others						
		At4g37010	calltractin-like protein	4.1	4.4E-04	4.1	5.9E-04
		At4g39890	small GTP-binding protein-like	3.0	3.0E-03	4.1	7.3E-04
Transcription							
	WRKY family protein						
		At2g23320	**putative WRKY-type DNA-binding protein (WRKY15)**	5.3	9.7E-05	5.1	1.2E-04
		At5g13080	WRKY-like protein (WRKY75)	6.5	3.8E-05	3.3	1.7E-03
		At4g23810	similar to WRKY transcription factor AR411 (WRKY53)	4.0	4.4E-04	4.4	2.9E-04
		At5g49520	similar to WRKY-type DNA binding protein (WRKY48)	3.4	1.4E-03	4.7	2.2E-04
		At2g30250	putative WRKY-type DNA binding protein (WRKY25)	3.4	1.2E-03	4.4	2.5E-04
		At1g62300	transcription factor WRKY6	4.5	2.4E-04	3.2	2.1E-03
		At5g22570	WRKY transcription factor 38 (WRKY38)	3.2	2.2E-03	3.3	3.1E-03
		At5g26170	WRKY transcription factor 50 (WRKY50)	3.1	2.2E-03	3.2	2.0E-03
	NAC family protein						
		At5g22380	NAC-domain protein-like (ANAC090)	3.3	1.7E-03	10.1	1.4E-05
		At2g17040	NAM (no apical meristem)-like protein (ANAC036)	3.5	1.0E-03	4.0	4.8E-04
	others						
		At1g27730	salt-tolerance zinc finger protein (Zat10)	5.7	7.0E-05	6.3	4.3E-05
		At5g59820	zinc finger protein Zat12	6.0	5.3E-05	5.5	7.7E-05
		At3g56710	SigA binding protein	4.5	2.2E-04	5.7	6.9E-05
		At3g46600	scarecrow-like 11 protein	3.2	1.9E-03	4.1	4.0E-04
		At1g18570	putative myb transciption factor (MYB51)	3.7	1.0E-03	3.2	2.4E-03
		At4g18880	**heat shock transcription factor 21 (AtHSF21)**	3.4	1.2E-03	3.2	1.9E-03
		At5g61010	putative protein	3.3	1.5E-03	3.3	1.6E-03
		At1g68840	putative DNA-binding protein (RAV2-like)	3.3	1.6E-03	3.1	2.3E-03
Defence Stress and Detoxification							
	disease resistance protein						
		At5g41750	**disease resistance protein-like**	5.9	5.7E-05	6.0	5.2E-05
		At1g57630	disease resistance protein RPP1-WsB, putative	5.9	5.7E-05	3.2	1.7E-03
		At5g41740	disease resistance protein-like	4.3	3.0E-04	4.4	2.7E-04
		At1g72900	virus resistance protein, putative	3.8	6.5E-04	3.9	5.1E-04
		At4g33300	similar to NBS/LRR disease resistance protein (RFL1)	3.5	1.1E-03	3.8	6.4E-04
	glutathione S-transferase						
		At1g17170	putative glutathione transferase	6.2	4.5E-05	6.0	5.1E-05
		At2g47730	glutathione S-transferase (GST6)	3.4	1.4E-03	3.4	1.3E-03
	others						
		At5g02780	putative protein, similar to In2	7.6	2.1E-05	5.7	7.4E-05
		At2g35980	similar to harpin-induced protein hin1 from tobacco	6.1	5.0E-05	5.0	1.3E-04
		At4g14630	germin precursor oxalate oxidase	5.1	1.2E-04	3.1	2.2E-03
Cellular Transport and Transport Mechanisms							
	ABC transporter						
		At1g15520	ABC transporter, putative	7.2	2.5E-05	3.3	1.4E-03
		At2g47000	putative ABC transporter	3.3	1.5E-03	4.0	4.4E-04
	calcium-ATPase						
		At3g63380	Ca2+-transporting ATPase-like protein	4.1	4.0E-04	3.7	7.0E-04
		At3g22910	calmodulin-stimulated calcium-ATPase, putative	5.3	9.4E-05	4.6	2.0E-04
	others						
		At4g21680	peptide transporter-like protein	3.3	1.6E-03	9.5	1.1E-05
		At4g35180	amino acid permease-like protein	5.4	8.9E-05	5.2	1.1E-04
		At2g13810	putative aspartate aminotransferase	6.3	4.6E-05	3.7	8.0E-04
		At5g26340	hexose transporter-like protein	4.2	3.4E-04	3.9	5.0E-04
		At3g52400	syntaxin-like protein syn14	3.6	9.2E-04	4.1	3.8E-04
		At5g61900	copine-like protein	3.1	2.4E-03	4.6	2.1E-04
		At5g40780	amino acid permease	3.7	6.7E-04	3.4	1.2E-03
		At1g08930	putative sugar transporter (ERD6)	3.1	2.6E-03	4.0	4.3E-04
Metabolism							
	UDP-glucose glucosyltransferase						
		At1g22400	UDP-glucose glucosyltransferase, putative	6.3	4.6E-05	3.1	2.5E-03
		At2g43820	putative glucosyltransferase	4.0	4.7E-04	3.6	9.2E-04
		At2g30140	putative glucosyltransferase	4.1	4.1E-04	3.5	1.1E-03
		At1g05560	UDP-glucose:indole-3-acetate beta-D-	4.1	4.0E-04	3.1	2.1E-03
		At4g34131	glucosyltransferase -like protein	3.3	1.6E-03	3.9	5.6E-04
	cytochrome p450 family						
		At3g26830	putative cytochrome P450	9.8	9.1E-06	4.5	2.2E-04
		At5g45340	cytochrome P450	3.7	9.3E-04	7.3	7.9E-05
		At4g37370	cytochrome P450-like protein	4.4	2.4E-04	3.9	5.4E-04
	FAD-linked oxidoreductase family						
		At5g44360	berberine bridge enzyme	4.3	2.9E-04	4.9	2.0E-04
		At4g20830	reticuline oxidase-like protein	4.3	3.1E-04	4.4	2.6E-04
		At4g20860	berberine bridge enzyme-like protein	3.7	7.0E-04	4.3	3.1E-04
	flavanone 3-hydroxylase-like protein						
		At5g24530	flavanone 3-hydroxylase-like protein	4.8	1.5E-04	4.3	3.0E-04
		At3g19010	oxidase like protein	3.5	1.0E-03	3.1	2.1E-03
	others						
		At3g22600	predicted GPI-anchored protein	8.1	1.6E-05	4.5	2.2E-04
		At4g25810	xyloglucan endo-1,4-beta-D-glucanase (XTR-6)	4.9	1.5E-04	6.7	3.3E-05
		At5g42830	N-hydroxycinnamoyl benzoyltransferase-like protein	5.6	7.4E-05	5.4	9.4E-05
		At2g26560	similar to latex allergen from Hevea brasiliensis	6.2	4.5E-05	4.7	1.7E-04
		At5g17330	glutamate decarboxylase 1 (GAD 1) (sp Q42521)	5.0	1.2E-04	5.1	1.1E-04
		At5g38900	fmE protein-like	5.1	1.2E-04	4.1	3.7E-04
		At5g51830	fructokinase 1	3.6	8.8E-04	5.2	1.1E-04
		At4g39830	putative L-ascorbate oxidase	3.6	9.5E-04	4.7	1.9E-04
		At4g00700	putative phosphoribosylanthranilate transferase	4.7	1.7E-04	3.3	1.5E-03
		At4g01700	putative chitinase	3.6	8.2E-04	3.6	9.2E-04
		At5g38710	proline oxidase, mitochondrial precursor-like protein	3.3	1.7E-03	3.9	1.3E-03
		At1g74710	isochorismate synthase (icsl)	3.7	7.2E-04	3.3	1.5E-03
		At5g19440	cinnamyl-alcohol dehydrogenase-like protein	3.4	1.2E-03	3.1	2.3E-03
DNA Synthesis and Processing							
		At2g32020	putative alanine acetyl transferase	3.3	1.6E-03	4.8	1.5E-04
		At5g01100	putative protein	3.6	1.3E-03	4.3	3.3E-03
		At4g39030	**enhanced disease susceptibility 5 gene (EDS5)**	4.0	4.5E-04	3.5	1.1E-03
Protein Fate							
		At5g60800	putative protein, similar to GMFP5	4.1	4.1E-04	8.6	1.5E-05
		At3g50930	BCS1 protein-like protein	5.2	1.1E-04	5.7	6.8E-05
Cellular Structural Organization							
		At5g64310	arabinogalactan-protein (gb AAC77823.1)	5.2	1.1E-04	4.6	2.0E-04
Energy							
		At1g32350	oxidase, putative	7.8	1.9E-05	3.7	7.1E-04
Protein Synthesis							
		At4g16680	RNA helicase	4.4	2.9E-04	3.7	1.7E-03
Unclassified Protein							
		At3g60420	**putative protein**	11.7	5.7E-06	14.1	3.9E-06
		At5g40990	GDSL-motif lipase hydrolase-like protein	12.0	6.3E-06	9.2	5.5E-05
		At1g19250	unknown protein	7.1	2.7E-05	6.6	3.6E-05
		At2g16060	class 1 non-symbiotic hemoglobin (AHB1)	5.6	7.2E-05	7.8	1.8E-05
		At5g11140	putative protein, similar to pEARLI 4	5.8	6.1E-05	5.4	9.0E-05
		At4g01870	predicted protein of unknown function	3.7	7.1E-04	6.9	2.9E-05
		At1g65500	unknown protein	4.4	2.6E-04	5.1	1.1E-04
		At1g22890	unknown protein	4.4	2.6E-04	4.6	2.0E-04
		At5g48410	ligand-gated ion channel protein-like (AtGLR1.3)	5.8	6.6E-05	3.4	2.5E-03
		At5g27420	RING-H2 zinc finger protein-like	4.7	1.9E-04	4.2	7.0E-04
		At3g14225	unknown protein	5.3	2.9E-04	3.5	3.9E-03
		At1g56060	hypothetical protein	6.1	5.3E-05	3.0	2.9E-03
		At4g22530	putative protein	4.3	2.9E-04	4.0	4.5E-04
		At5g49700	putative protein	3.4	1.2E-03	5.0	2.0E-04
		At5g48400	ligand-gated ion channel protein-like; glutamate receptor-	5.0	1.3E-04	3.2	2.1E-03
		At1g55450	hypothetical protein	3.6	8.5E-04	4.3	2.9E-04
		At4g40020	putative protein, similar to myosin heavy chain	3.5	1.4E-03	4.5	9.6E-04
		At5g63230	putative protein	3.8	8.4E-04	3.9	6.2E-03
		At2g46600	polygalacturonase inhibiting protein 1; PGIP1 (gb	3.4	1.2E-03	3.8	6.1E-04
		At1g16420	hypothetical protein	3.9	5.8E-04	3.1	2.2E-03
		At4g12720	growth factor like protein	3.8	6.0E-04	3.1	2.6E-03
		At1g23710	unknown protein	3.5	1.0E-03	3.3	1.7E-03
		At1g63840	putative RING zinc finger protein	3.7	7.5E-04	3.1	2.6E-03
		At5g64000	3(2),5-bisphosphate nucleotidase (SAL2)	3.0	3.2E-03	3.7	1.9E-03
		At4g38540	monooxygenase 2 (MO2)	3.0	2.7E-03	3.7	8.3E-04
		At4g24160	putative protein	3.1	2.5E-03	3.5	1.0E-03
		At5g62180	putative protein, similar to PrMC3	3.0	2.8E-03	3.3	3.2E-03
		At5g52810	putative protein	3.1	2.3E-03	3.0	2.8E-03

Ten-day-old seedlings of wild type and *atnfxl1* mutant plants were grown MS plates and harvested after 1 μM T-2 toxin treatment for 24 hr
Genes in bold-face: expression was verified by real time RT-PCR (see Table 3).
[A]Classification of functional category was based on information from the Munich Information Center for Protein Sequence (MIPS).
[B]Upregulated genes were designated as such based on a 3-fold or greater change (FC) in the normalized signal between T-2 toxin-treated *atnfxl1* m
[C]All of these changes in gene expression were statistically significant, with at P<0.01.

Table 2. Downregulated genes in the T-2 toxin-treated *atnfxl1* mutant plants compared to T-2 toxin-treated w

		exp.1		exp.2	
AGI code	Descriptions	FC[a]	P value[b]	FC	P value
At4g19170	neoxanthin cleavage enzyme-like protein	0.164	5.6E-03	0.073	2.0E-03
At4g16830	nuclear antigen homolog	0.111	3.3E-03	0.164	5.7E-03
At5g50950	fumarate hydratase	0.150	4.8E-03	0.137	4.3E-03
At5g23010	2-isopropylmalate synthase-like	0.206	8.7E-03	0.090	2.5E-03
At4g13770	cytochrome P450 monooxygenase (CYP83A1)	0.193	7.7E-03	0.111	3.2E-03
At5g07690	**myb family transcription factor (MYB29)**	0.200	8.7E-03	0.116	3.6E-03
At1g14250	nucleoside phosphatase family protein / GDA1/CD39 family protein	0.200	8.3E-03	0.128	4.0E-03
At5g03760	glycosyl transferase family 2 protein	0.161	5.8E-03	0.174	7.3E-03
At4g21650	subtilisin proteinase - like	0.206	8.9E-03	0.151	5.0E-03
At3g27690	chlorophyll A-B binding protein (LHCB2:4)	0.196	7.9E-03	0.164	5.6E-03
At5g12250	tubulin beta-6 chain	0.189	7.3E-03	0.186	7.2E-03
At4g21960	peroxidase 42 (PER42)	0.217	9.8E-03	0.199	8.1E-03

Ten-day-old seedlings of wild type and atnfxl1 mutant plants were grown MS plates and harvested after mock or 1 μM T-2 toxin treatment f
The expression of MYB29 (bold-face) was verified by real time RT-PCR analysis (see Table 3).
[a]Downregulated genes were designated as such based on a 3-fold or greater change in the normalized signal of T-2 toxin-treated *atnfxl1* n
[b]All of these changes in gene expression were statistically significant, with at P<0.01.

Table 3. Validation of microarray results in the 1μM T-2 toxin-treated plants by real time PCR.

	Fold change (*atnfxl1* mutant *vs* wild type)		
AGI code	Microarray[a]	real time PCR[b]	Description
Upregulated Genes			
At5g25930	4.00	11.6±1.39	receptor protein kinase-like protein
At2g23320	5.17	4.87±0.26	putative WRKY-type DNA-binding protein (WRKY15)
At4g18880	3.30	5.21±0.68	heat shock transcription factor 21 (AtHSF21)
At5g41750	5.97	12.08±1.56	disease resistance protein-like
At4g39030	3.76	7.52±1.04	enhanced disease susceptibility 5 gene (EDS5)
At3g60420	12.84	11.56±2.16	putative protein
Downregulated genes			
At5g07690	0.15	0.12±0.02	Myb family transcription factor (MYB29)

Ten-day-old seedlings of wild type and *atnfxl1* mutant were grown MS plate and harvested after 1 μM T-2 toxin trea

[a]Fold change in microarray results is the average value of two arrays.

[b]Fold change in real time PCR is an average value of four independent biological sample sets.

Figure legends

Figure 1. An *atnfxl1* mutant (*atnfxl1-1*) is hypersensitive to type A trichothecenes. (a) Schematic diagram of *AtNFXL1* in *Arabidopsis thaliana*. Boxes indicate exons. The organization of the exon-intron boundary was predicted by the nucleotide sequence of the full length cDNA, and is identical to our results. The T-DNA insertion site is indicated by a triangle. Two different regions (basepairs 120-438 and 2368-3568) of *AtNFXL1* for RT-PCR analysis is indicated by thick lines. (b) A truncated transcript of *AtNFXL1* was observed in the *atnfxl1-1* mutant. Ten-day-old seedlings of wild type and *atnfxl1-1* mutant plants were grown on MS plates and harvested after mock treatment, or 1 μM T-2 toxin treatment for 24 hr. Total RNA was prepared from the seedlings and used for RT-PCR analysis. Two different regions (basepairs 120-438 and 2368-3568) of *AtNFXL1* were amplified by specific primer sets. *Actin2/8* was used as a loading control. (c) Representative photographs of wild type, *atnfxl1*, and complementation plant lines that were mock-treated (upper row), or treated with 0.1 μM T-2 toxin (lower row). Sterile seeds were sown on MS medium with or without 0.1 μM T-2 toxin, and then stratified for 2 d at 4ºC in the dark. Plants were grown for 8 days in a growth chamber,

and then photographed. Scale bars = 1 cm. (d) The fresh weight of each plant is expressed relative (%) to mock-treated wild type. Plants were treated with 0.1 μM T-2 toxin or 10 μM DON without trichothecenes, as stated above. *atnfxl1:PAtNFXL1::AtNFXL1* (line #5) refers to an *atnfxl1* mutant carrying an *AtNFXL1 promoter::AtNFXL1* gene fusion. Data is representative of two independent experiments. *, $P < 0.01$, based on the Student's *t*-test. Similar results were obtained in other six independent complementation lines.

Figure 2. *AtNFXL1* is involved in SA biosynthesis and expression of SA-related genes. Eight-day-old plants were either mock-treated or treated with 1 μM T-2 toxin for 24 hr and then subjected to Real time PCR analysis (a) or SA quantification (b-c). (a) Real time PCR analysis of *PR-1* and *ICS1* of *atnfxl1* mutant and wild type plants. Total RNA was isolated from each sample and then subjected to Real time PCR analysis. The levels of mRNA were determined by real-time RT-PCR, and normalized with that of *Actin2/8*. Expression levels are relative to that of mock-treated wild type samples. Data is the average of three independent samples. Error bars indicate the standard deviation. (b-c)

Enhanced accumulation of SA in T-2 toxin-treated *atnfxl1* mutant plants. (b) Free and (c) total SA levels were quantified by high-performance liquid chromatography (data represents the means ± standard deviation, n=4).

Figure 3. GUS staining and quantification of GUS activity in *AtNFXL1 promoter::GUS* stable transformants in response to elicitor, phytohormone, or trichothecene treatment. GUS staining of mock- (a), T-2 toxin- (b) or SA-treated 8 day old plants (c). Sterile seeds were sown on MS agar medium with 0.1 μM T-2 or 100 μM SA, and then stratified for 2 d at 4ºC in the dark. Plants were grown for 8 days in a growth chamber, and then subjected to GUS staining. Scale bars = 1 mm. (d) Quantification of GUS activity in *AtNFXL1 promoter::GUS* stable transformants treated with the indicated substances. Plants were grown for 8 days on MS agar medium in a growth chamber, and then either mock-treated or treated with the indicated substance for 24 hr and used for quantitative GUS assays. GUS activity in treated samples relative to mock-treated samples was measured using a fluorometric GUS assays (n=4). Data is representative of two independent experiments.

Figure 4. Reduced susceptibility of *atnfxl1* mutant plants to the compatible pathogen *Pst* DC3000. (a) Leaves of *atnfxl1* mutant (closed circles) and wild type (open circles) plants were collected 0, 1, 2 and 4 days post-inoculation and homogenized in 10 mM $MgCl_2$. The number of colony-forming units (CFU) was estimated by growth on nutrient broth agar plates after the appropriate dilution. Data represents the averages ± standard deviation (n=6). A significant difference between wild type and *atnfxl1* mutant plants was observed in the number of CFU/g fresh weight ($p<0.05$, ANOVA). Data is representative of two independent experiments. (b) Complementation analysis of the reduced susceptibility to *Pst*DC3000 in an *atnfxl1* mutant. Leaves of wild type, *atnfxl1*, and complementation plant line were collected 2 days post-inoculation. Data represents the averages ± standard deviation (n=6). A significant difference between the number of CFU/g fresh weight of *atnfxl1* mutant plants and wild type/complementation line #4 plants was observed ($p<0.05$, ANOVA). Similar results were obtained in complementation lines #1 and #3.

Figure 5. Model of opposing functions of *AtNFXL1* in biotic and abiotic stress response. Biotic stress often causes accumulation of elicitors and/or SA in host plants. SA and elicitors including T-2 toxin induce the expression of *AtNFXL1*. An *atnfxl1* mutant exhibits a hypersensitivity phenotype to T-2 toxin due to excessive defense responses. *AtNFXL1* functions as a negative regulator of defense-related genes via an SA-dependent signaling pathway, which resulting in reduced susceptibility to a virulent pathogen, *Pst* DC3000 in the *atnfxl1* mutant. Abiotic stress such as salt and osmotic stress also induces the expression of *AtNFXL1* (Lisso *et al*., 2006). *AtNFXL1* functions as a positive regulator of salt-responsive genes (Lisso *et al*., 2006). The *atnfxl1* mutant exhibited a reduced survival rate under salt stress (Lisso *et al*., 2006).

Supplemental Figure 1. AtNFXL1 belongs to the NF-X1 family of proteins.

(a) Schematic diagram of AtNFXL1 in *Arabidopsis thaliana* (Accession no. AAD32867) and comparison of AtNFXL-1 with the following homologues: OsNF-X1, *Oryza sativa* (Accession no. BAD46154); NF-X1, *Homo sapiens* (Accession no. NP_002495); STC, *Drosophila melanogaster* (Accession no. NP_476599); Fap1,

Saccharomyces cerevisiae (Accession no. NP_014375). The purple regions indicate the NLS; red and blue indicate the RING-CH finger domain and the nine NF-X1-type Zn finger domains, respectively; green indicates the R3H domain. (b) A rooted maximum-likelihood phylogenetic tree of AtNFXL1 and AtNFXL1 homologues. DrNF-X1, *Danio rerio* (Accession no. XP_690559); MmNF-X1, *Mus musculus* (Accession no. AAF34700); CeNF-X1, *Caenorhabditis elegans* (Accession no. NP_498394); and SpNF-X1, *Schizosaccharomyces pombe* (Accession no. CAA21417). (c) Alignment of the amino acid sequences of the nine AtNFXL1-type Zn finger domains. The number to the left of each repeat indicates its position in the AtNFXL1 protein sequence. The consensus sequence for the Zn finger repeat is shown above the sequences, and is based on matches in seven of the nine aligned sequences.

Supplemental Figure 2. Subcellular localization of GFP-AtNFXL1 and GFP proteins in *Arabidopsis* cells. Protoplasts of *Arabidopsis* T87 suspension culture cells were transfected using the polyethylene glycol (PEG) method. GFP-AtNFXL1 fusion protein localized to the nucleus of *Arabidopsis* cells (a-c). In contrast, GFP localized to the

cytosol (d-f). GFP fluorescence was visualized in using a fluorescence microscope.

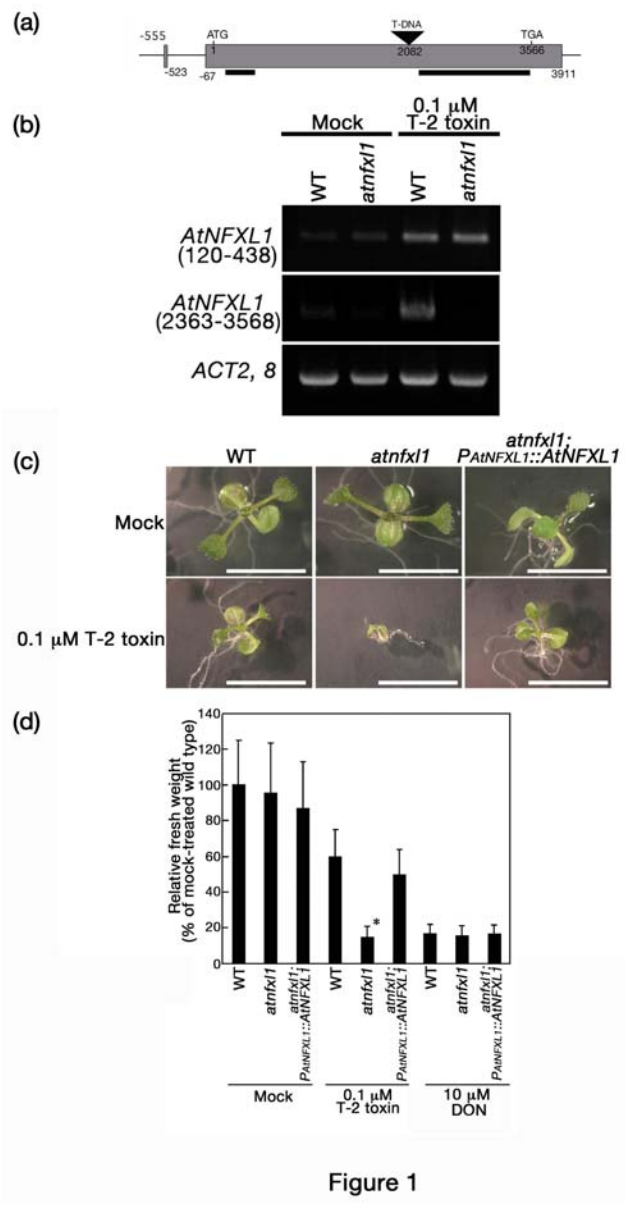

Figure 1

111x213mm (400 x 400 DPI)

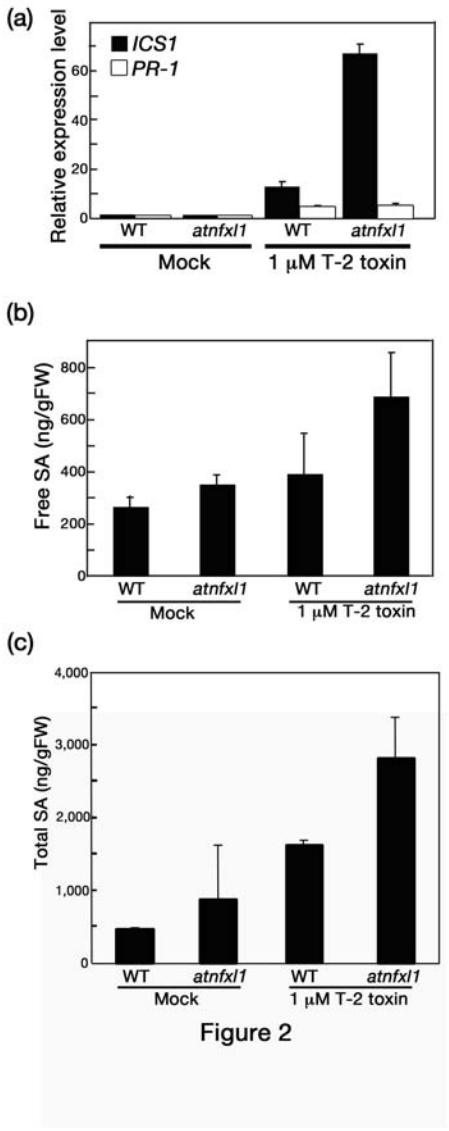

Figure 2

100x210mm (400 x 400 DPI)

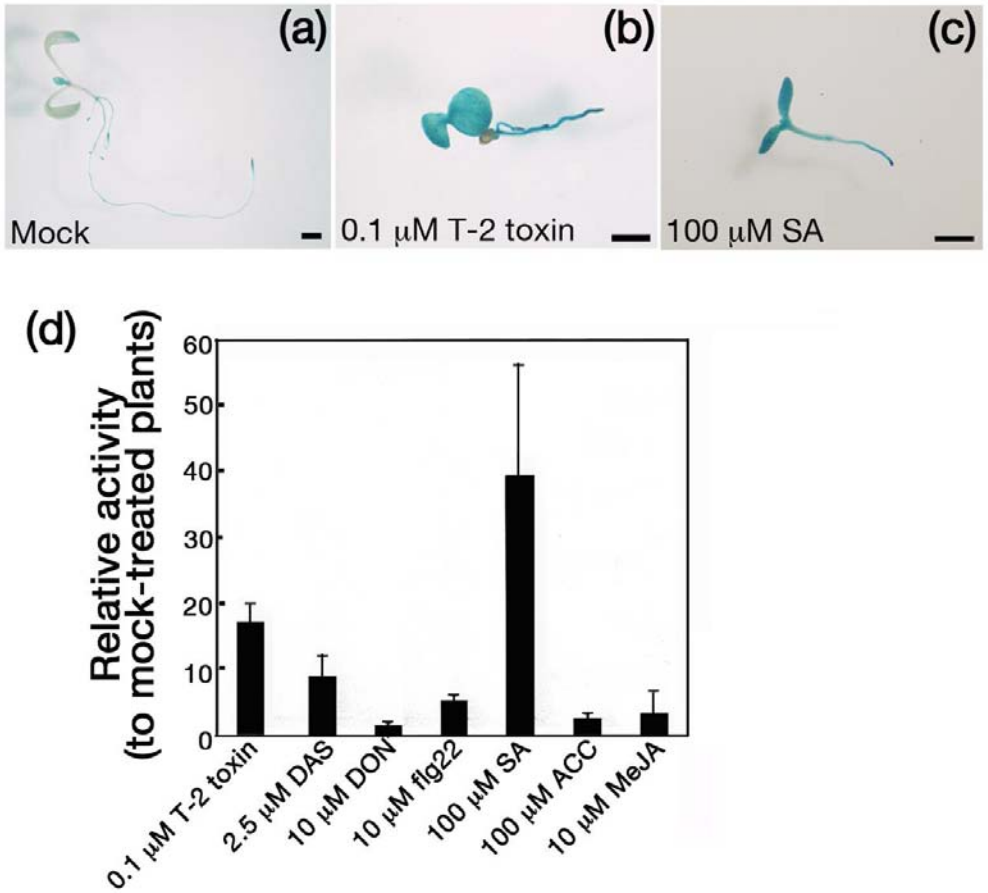

Figure 3

80x82mm (400 x 400 DPI)

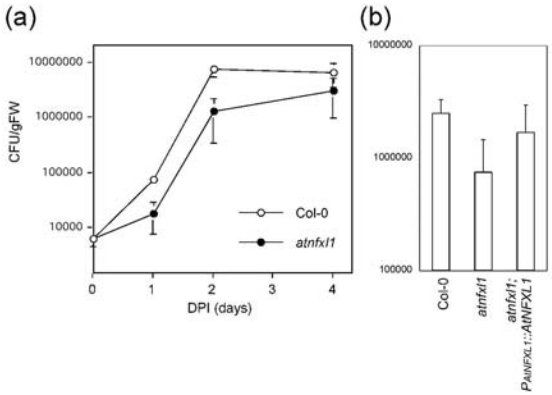
(a)
(b)
CFU/gFW
10000000
1000000
100000
10000
0
1
2
3
4
DPI (days)
Col-0
atnfxl1
Col-0
atnfxl1
atnfxl1::AtNFXL1
PAtNFXL1::AtNFXL1

Figure 4

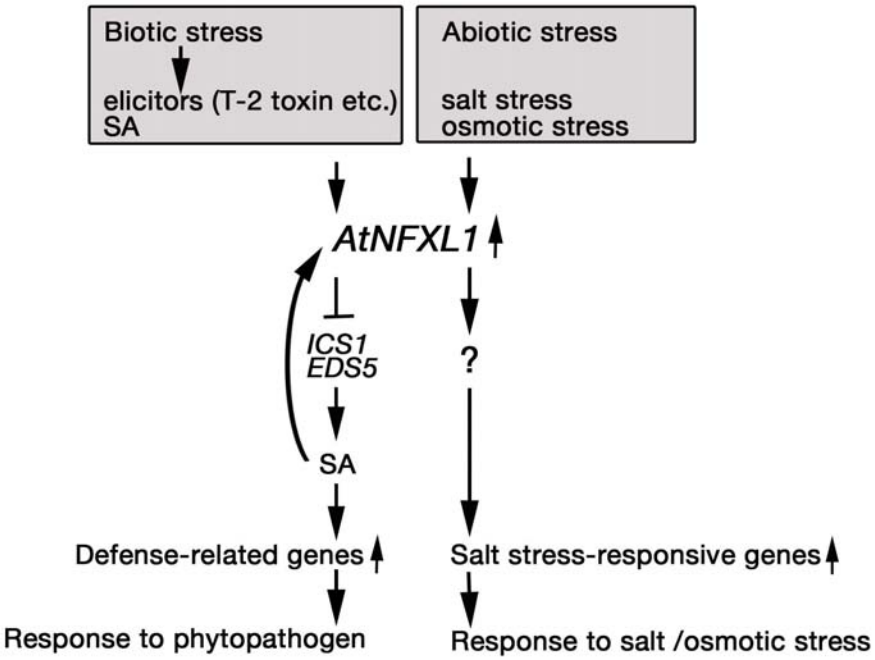

Figure 5

120x109mm (400 x 400 DPI)